Full Paper

Journal of the Brazilian Chemical Society

https://dx.doi.org/10.21577/0103-5053.20250185

J. Braz. Chem. Soc. **2026**, *37*, e-20250185, 1-10

Phagocytosis Modulated by a Pt^{II} Complex with Triphenylphosphine and 5-Heptyl-1,3,4-oxadiazole-2-(3*H*)-thione in a Microemulsion System

Bruna A. Rodrigues, [a] ***Angelina M. de Almeida,*** [b] ***Mauro V. de Almeida,*** [b] ***Jackson Antônio L. C. Resende,*** [a] ***Wendell Guerra,*** [c] ***Eduardo L. França,*** [d] ***Aron Carlos de M. Cotrim*** [d] ***and Wesley A. Souza*** *,[a]

[a]*Instituto Ciências Exatas e da Terra, Universidade Federal de Mato Grosso, 79698-00 Pontal do Araguaia-MT, Brazil*

[b]*Departamento de Química, Universidade Federal de Juiz de Fora, Campus Martelos, 36036-900 Juiz de Fora-MG, Brazil*

[c]*Instituto de Química, Universidade Federal de Uberlândia, Campus Santa Mônica, 38400-902 Uberlândia-MG, Brazil*

[d]*Instituto Ciências Biológicas e da Saúde, Universidade Federal de Mato Grosso, 78605-091 Barra do Garças-MT, Brazil*

In this work, the *trans*$[Pt(L)_2(PPh_3)_2]$ complex (L: 5-heptyl-1,3,4-oxadiazole-2-(3*H*)-thione) was associated with a microemulsion (ME/Pt^{II} complex). The microemulsified system underwent physicochemical characterization, including pH, conductivity, rheology, zeta potential, and dynamic light scattering (DLS) measurements. The microemulsion system remained stable at a pH near 6.0, indicating biocompatibility, while the conductivity was between 7 and 8 μS cm^{-1}, with a hysteresis area of −0.06 Pa s^{-1} for the ME/Pt^{II} complex. The DLS technique confirmed the presence of a microemulsion with particle sizes ranging from 10 to 200 nm. The polydispersity index for the ME/Pt^{II} complex system was close to 0.3, indicating a monodisperse system, with a zeta potential of −19.2 ± 4.49 mV. These results showed that the system containing the Pt^{II} complex and the microemulsion is thermodynamically stable. Subsequently, cell viability studies demonstrated that the ME/Pt^{II} complex system is not toxic to peripheral blood mononuclear cells (PBMCs). In the phagocytosis activity assay, the complex associated with the microemulsion showed an increase in the phagocytosis index, suggesting that the microemulsion (ME/Pt^{II} complex) has potential for new biological assays, such as antitumor and antibacterial.

Keywords: Pt^{II} complexes, microemulsion, zeta potential, phagocytosis activity, cell viability, immunomodulatory

Introduction

The discovery of the antitumoral properties of cisplatin by Rosenberg *et al.*[1] provided a major advance in the treatment of several types of cancer, including testicular, ovarian, lung, head, stomach, esophagus, neck, lymphomas, osteosarcoma, melanoma, breast, and cervix.[1-3] Despite the success of cisplatin in clinical medicine, it has several side effects, such as nephrotoxicity, cumulative peripheral sensory neuropathy, ototoxicity, nausea, and vomiting, as well as resistance, intrinsic or acquired.[4] As a consequence, the development of new platinum-based drugs has been performed, and some of them are widely used in clinical medicine, namely carboplatin, oxaliplatin, nedaplatin, lobaplatin, and heptaplatin.[5-8]

In recent decades, in addition to developing new drugs, research and development of new pharmaceutical formulations have been highlighted to achieve better selectivity and efficacy, thereby reducing the side effects of chemotherapy drugs.[4,9] In this sense, a type of formulation that has aroused interest is microemulsions (ME), which have droplets with a diameter of less than 150 nm, usually in the order of 100 nm, which are formed by droplets small enough to be visually transparent. As a result, other names, such as sub-microemulsion and nanoemulsion, are used to describe

*e-mail: wesley.souza@ufmt.br
Editor handled this article: Célia M. Ronconi (Associate)

this modified system, which is thermodynamically stable and offers several advantages, including ease of manufacturing and greater solubility.[10,11] Also, microemulsions may have greater bioavailability when administered orally, allowing reduced medication doses. Such characteristics reduce side effects and toxicity.[11-15] For example, in a study developed by Akartas and Karasulu,[14] in which a self-microemulsifying drug delivery system (SMEDDS) was prepared, namely Cisplatin SMEDDS, the results from *in vitro* studies resulted in the release of 78.17% of cisplatin, which shows promising cytotoxic activity in the A2780 cell line, and could be an alternative for the treatment of ovarian cancer. According to the results presented, the Cisplatin SMEDDS formulation proved more effective than the cisplatin solution and demonstrated better lymphatic targeting. It can be administered orally in hard gelatin capsules.[14,16]

In addition to the research and design of new platinum complexes as anticancer agents, significant effort has been invested in evaluating the microbicidal potential of this class of compounds, mainly due to the rise in bacterial resistance to conventional antibiotics, which has led to a significant increase in deaths.[16-18] In the study conducted by Lacerda *et al*.[17] on antimicrobial resistance in *Campylobacter jejuni*, a platinum(II) complex with the ligand 5-amino-1,3,4-thiadiazole-2(3*H*)-thione in combination with ciprofloxacin (CIP), reduced the minimum inhibitory concentration (MIC) to 0.25, 0.5, and 2 mg L^{-1}. Combined with erythromycin (ERY), a significant MIC reduction was observed in only one strain, where the MIC decreased from 32 to 0.25 mg L^{-1}. Another example, platinum cyclooctadiene complexes Pt1 and Pt2, were very active against gram-positive *Staphylococcus aureus* with MIC values close to (3.125 and 1.56-3.125 μg mL^{-1}).[19]

Interestingly, oxadiazole derivatives exhibit several biological activities, including antifungal, antibacterial, anticancer, anti-inflammatory, and antiviral.[20,21] As can be seen in the studies carried out by Unadkat *et al*.,[22,23] who performed a sampling based on molecular dynamics in which a series of 1,2,4-oxadiazole derivatives were applied in cytotoxicity assays in several tumor cell lines such as overexpressing Epidermal Growth Factor Receptor (EGFR) (A549, HCT-116, HEPG2, MCF-7) and one EGFR negative cancer cell line (SW620), of which some compounds stood out with half-maximal inhibitory concentration (IC_{50}) in the micromolar range. A recent study[24] involving the development of cerium oxide nanoparticles decorated with triethyl phosphine (CeNPs-TEP) proved to be an alternative in the development of new anti-leishmania chemotherapeutic agents since the generation of reactive oxygen species (ROS) had an increase of approximately 2.2 times inside the cells of *Leishmania donovani* Ag83, induced by the presence of CeNPs-TEP, which caused the death of approximately 60 to 82% through the exposure time that was 24 and 48 h, respectively. Another interesting example is the Pt^{II}-3-hydroxy-2-tolyl-4*H*-chrome-4-one complex (Pt^{II}-HToC), which showed greater bactericidal efficacy than a common antibiotic. Its MIC values are 0.162/100 μL, demonstrating remarkable antibacterial activity.[25]

The rationale for developing complexes with the ligand triphenylphosphine is based on reports suggesting that they may exhibit different mechanisms of action than cisplatin.[26,27] The *trans*-$[Pt(L)_2(PPh_3)_2]$ complex is shown in Figure 1, whose synthesis and characterization are described in the literature.[3] Since the complex studied here is insoluble in pure dimethyl sulfoxide (DMSO), it is impossible to use the protocols commonly used for biological assays.[28] The application of the *trans*-$[Pt(L)_2(PPh_3)_2]$ (L = 5-heptyl-1,3,4-oxadiazole-2-(3*H*)-thione) complex in this study is based both on its structural and chemical aspects and on the wide application of platinum complexes in medicine, especially in antitumor chemotherapy, where compounds such as cisplatin have a consolidated history of clinical efficacy. The *trans* configuration offers a differentiated structure capable of influencing essential properties, such as lipophilicity, interactions with biomolecules, and cell permeability, which are decisive aspects in the search for new platinum compounds with an improved pharmacological profile and reduced toxicity compared to conventional drugs. To overcome the low solubility of the complex in biological solvents, a microemulsified system was adopted, enabling verification of its solubility and dispersion and allowing the performance of biological assays focused on the immunomodulatory capacity of the compound, expanding its therapeutic potential.

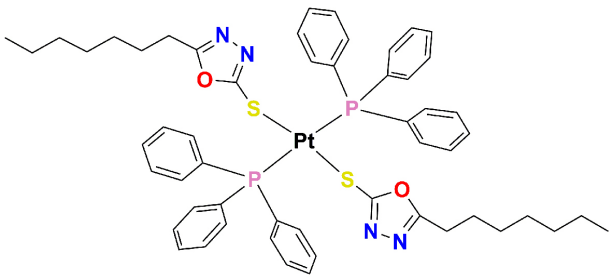

Figure 1. Chemical structure of Pt^{II} complex *trans*-$[Pt(L)_2(PPh_3)_2]$.

Experimental

Chemical reagents

In this work, distilled water, capric/caprylic acid triglycerides (Polymol 812, hydrophilic-lipophilic balance (HLB) 10.8; Emfal, Betim, MG, Brazil), sorbitan

oleate (Span 80, SP, HLB 4.3; Emfal, Betim, MG, Brazil), polysorbate 80 (Tween 80, TW, HLB 15.0; Vetec Química Fina, Rio de Janeiro, RJ, Brazil), and 1-butanol (BT; Vetec Química Fina, Rio de Janeiro, RJ, Brazil) were used. The *trans*-[Pt(5-heptyl-1,3,4-oxadiazole-2-thione)$_2$(PPh$_3$)$_2$] complex used in this study was provided by the LASFAR research group of the Institute of Chemistry, Federal University of Uberlândia. It was previously synthesized and characterized as described in the literature.[3] Ficoll-Paque Plus density gradient medium (Pharmacia-Uppsala, Sweden), phosphate-buffered saline (PBS, pH 7.4), orange acridine dye, and tubes containing ethylenedinitrilotetraacetic acid (EDTA) anticoagulant were also employed for washing and cell analysis.

Microemulsion system

The microemulsions (MEs) were prepared using distilled water, caprylic/caprylic acid triglycerides - Polymol 812, with HLB of 10.8, sorbitan oleate - Span 80 (SP) with HLB of 4.3, polysorbate 80 Tween 80 (TW) with HLB of 15.0 and 1-butanol (BT), the system was designated SP/TW/BT as described in the literature.[15]

To achieve the HLB required by the oil phase, the determination of the fractions of the surfactant mixture, the HLBs of SP and TW surfactants were considered (Cotrim *et al.*),[29] according to the equations:

$$HLB_r = \frac{HLB_{T_1} \times HLB_{T_2} \times F_{T_2}}{10 - (F_c)} \quad (1)$$

$$F_{T_1} + F_{T_2} + F_C = 10 \quad (2)$$

where HLB_r represents the HLB required by the oil phase; HLB_{T1}, the HLB of surfactant 1; HLB_{T2}, the HLB of surfactant 2; F_{T1}, the fraction of surfactant 1; F_{T2}, the fraction of surfactant two, and F_C, the fraction of co-surfactant ($F_C = 1$).[15,29]

To act as a co-surfactant, BT was used at a rate of 10% of the surfactant mixture, as it did not present an HLB value, and the percentage of SP and TW surfactants was calculated to achieve the HLB required by capric acid triglyceride/caprylic as shown in Table S3 (Supplementary Information (SI) section). The fraction of the SP/TW/BT surfactant mixture resulted in the HLB required by the oil phase in the fraction of 3.5:5.5:1.0.[15,29]

Association of the complex *trans*-[Pt(L)$_2$(PPh$_3$)$_2$] into microemulsion

Initially, the oil phase was prepared with 0.0100 g of the complex *trans*-[Pt(L)$_2$(PPh$_3$)$_2$], previously synthesized and characterized, by the techniques of elemental analysis, high resolution mass spectrometry, infrared spectroscopy, nuclear magnetic resonance (NMR) ^{1}H, ^{13}C, ^{31}P and ^{195}Pt as described in the literature,[3] in 1.00 mL of capric/caprylic acid, 0.200 mL of BT, 0.200 mL of SP, and 0.200 mL of TW, were mixed and left at room temperature for 24 h.

0.5029 g of previously prepared oils, 0.8124 g of SP, and 1.2941 g of TW were used to prepare the microemulsion. After these additions, the first homogenization was performed under vigorous stirring. Then, we added 0.4500 g of distilled water in two steps: 0.2000 g, followed by 0.2500 g. Finally, we added 0.1749 g of BT. Each step was homogenized before the addition of the next formulation component (see Figures S5).

Characterization of microemulsion complex *trans*-[Pt(L)$_2$(PPh$_3$)$_2$] associated

To evaluate the physicochemical characteristics and thermodynamic stability of the microemulsion systems containing the *trans*-[Pt(L)$_2$(PPh$_3$)$_2$] complex, rheological, electrical conductivity, dynamic light scattering (DLS), and zeta potential analyses were carried out.

The rheological parameters were determined on a Modular Compact Rheometer (MCR 102; Anton Paar GmbH, Ostfildern, Germany) of cone-plate type. The microemulsion (700 μL) was added to the plate surface at the adjusted temperature and maintained at 25 °C. The readings were carried out with permanent control of the measurement gap using TruGap support at 0.099 mm, a Toolmaster CP 50 measuring cell, and precise temperature control via the T-Ready feature with Rheoplus Software V3.61. The flow and viscosity curves were obtained using shear stress (τ) as a parameter for the test, varying from 0 to 5 mPa s for the ascending curve and from 5 to 0 mPa s for the descending curve.[29]

Electrical conductivity was evaluated using a bench conductivity meter (model CD12, BEL Engineering, Monza, Italy), calibrated with a standard KCl 0.1 mol L^{-1} solution, with an electrode inserted directly into the sample.[29]

The pH values were obtained using a digital benchtop pH meter model mPA-210 (MS Tecnopon), with a glass electrode calibrated with standard buffers of pH 4.0, pH 7.0, and pH 10.0.[29]

DLS and zeta potential were obtained using a ZetaSizer Nano (Malvern Instruments). The dimensions of suspended particles were measured at 25 °C and excited at 633 nm. The solvent used for this characterization was distilled water, and the microemulsion had a refractive index of 1.44 and

an absorption at 0.190 nm. The samples were suspended using a 1:100 dilution of the MEs.

Cellular viability assay

The present study was submitted and approved by the Research Ethics Committee of the Federal University of Mato Grosso (protocol number: 27068719.1.0000.5587).

Cell viability and phagocytosis index were performed on Peripheral Blood Mononuclear Cells (PBMC) separated by the density gradient technique using Ficoll-Paque (Pharmacia-Upsalla Sueder). Blood samples were obtained from 10 healthy donors aged 20-50 years, and 8 mL of blood were collected in tubes containing EDTA anticoagulant. Blood samples were centrifuged at 1500 rpm for 40 min in tubes containing 3 mL Ficoll-Paque Plus. The PBMC ring was removed, separated, and washed twice in phosphate buffer saline (PBS), pH 7.4. Cells were counted in a Neubauer chamber, and concentrations were adjusted to 2×10^6 cells mL^{-1}.[30]

500 µL of PBMCs and 5 µL of microemulsion, with or without the Pt compound, were combined and incubated for 30 min at 37 °C to assess viability. After this period, the samples were centrifuged for 10 min at 1500 rpm. The cell pellet was suspended in 200 µL of acridine orange for 1 min, then washed and centrifuged twice with PBS. Then, the slides were mounted for counting under a fluorescence microscope (Nikon Eclipse E 200, Nikon Corporation, Tokyo, Japan). Viability studies are reported as percentages based on a count of 100 cells, with cells classified as alive if colored green and dead if colored orange.[30]

Phagocytosis activity assay

The phagocytosis index was determined by incubating PBMCs with enteropathogenic *Escherichia coli* (EPEC). The EPEC stock culture is maintained in semisolid agar at room temperature in the absence of light. The adjusted bacterial concentration to 1.00×10^7 mL^{-1} was measured in a spectrophotometer at 620 nm (0.1-0.2). After adjustment, we prepared a 20% bacteria solution to 80% PBS.[15,30,31]

Volumes of 500.0 µL of bacterial suspension, 500.0 µL of cell suspensions (mononuclear phagocytes), and 5.0 µL of microemulsions incorporated and not incorporated into the Pt^{II} complex were mixed in Falcon-type centrifuge tubes and subjected to incubation for 30 min under shaking at 37 °C.[15,30,31]

After incubation, phagocytosis was stopped by adding ice-cold PBS, and the suspension was centrifuged for 10 min at 1500 rpm. The pellet was stained with 200.0 mL of orange acridine for 1 min, resuspended in PBS, centrifuged, and washed twice. Then, the slides were prepared, and the cells were counted using a fluorescence microscope (Nikon-Eclipse E200).[15,30,31]

Phagocytosis activity was evaluated using the acridine orange method, represented as a percentage based on the count of 100 cells. The cells counted are classified into live cells (green) with live bacteria inside and live cells (green) with dead bacteria (orange) inside, with the parameters obtained by the equation 3.[15,30,31]

$$\text{Phagocytosis index (\%)} = \frac{\left(\begin{matrix}\text{Number of}\\ \text{phagocytosis}\end{matrix}\right) + \left(\begin{matrix}\text{phagocytosis with}\\ \text{dead bacteria}\end{matrix}\right)}{100} \times 100 \quad (3)$$

Results and Discussion

Association of the complex *trans*-$[Pt(L)_2(PPh_3)_2]$ into microemulsion (ME/Pt^{II} complex system)

The microemulsion system utilized in this study is thoroughly described and discussed in the literature.[29] The microemulsion with associated platinum(II) complex (ME/Pt^{II} complex), whose concentration is 8.71×10^{-4} g mL^{-1}, and the unincorporated microemulsion (ME) presented pH and conductivity measurements at 25 °C as shown in Table 1.

Table 1. Measured pH and conductivity values of microemulsions (ME)

	pH	Conductivity / (µS cm^{-1})
ME	6.42 ± 0.05	7.11 ± 0.24
ME/Pt^{II} complex	6.47 ± 0.4	8.02 ± 0.33

Analyze significant statistics when the p-value is less than 0.05 ($p < 0.05$).

The pH values obtained for the formulations remained close to 6.5, indicating biocompatibility, as physiological pH typically ranges from 4.5 to 7.4. Moreover, the electrical conductivity of the ME/Pt^{II} complex remained stable at approximately 8.0 µS cm^{-1}. These findings are relevant for determining the nature of the dispersion in the microemulsion system.[32] Based on the conductivity value exceeding 1.40 µS cm^{-1}, the formulation can be classified as an oil-in-water (O/W) type microemulsion, in which the oily phase constitutes the dispersed (discontinuous) phase and water serves as the continuous (dispersing) phase.[10,29,33]

Rheological characterization studies the flow behavior and deformation of materials such as liquids, gels, polymers, pastes, and suspensions. This process offers valuable insights into the rheological and viscoelastic properties of materials. When the values fall between −1 Pa s^{-1} and +1 Pa s^{-1}, the hysteresis area indicates that

the materials exhibit Newtonian rheological behavior. This characterization involves studying the flow behavior and deformation of liquids, gels, polymers, pastes, and suspensions. Moreover, values between −0.2 Pa s^{-1} and +0.2 Pa s^{-1} indicate a stable Newtonian pattern.[29]

The behavior of the flow curves of the microemulsions starts from the origin without varying viscosity with shear stress, thus indicating a Newtonian flow profile, presenting a hysteresis area of −0.06 Pa s^{-1} for the Pt^{II} complex associated with ME and 0.66 Pa s^{-1} for the non-associated ME, as shown in Figure 2.

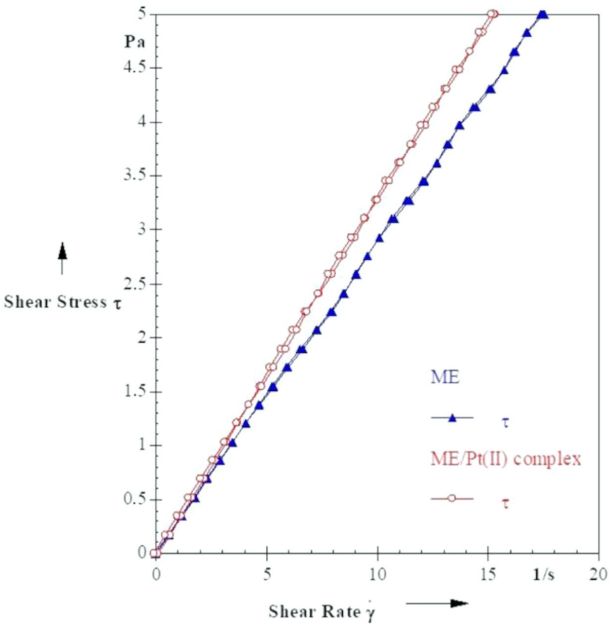

Figure 2. Flow curve of the microemulsion (ME) and the Pt^{II} complex associated with the microemulsion (ME/Pt^{II} complex) at 25 °C.

The viscosity showed minimal variation with increasing shear rate, displaying linear curves with different values and a slight increase when associated, which indicates that the association of the complex alters the viscosity parameters of the microemulsion, as illustrated in Figure 3.

The association of the complex Pt^{II} alters the rheological parameters of the microemulsion without altering the behavior, maintaining the linearity of the curves. Initially observed as Newtonian and presents greater stability when compared to the non-associated microemulsion, according to studies that indicate that the value of the low hysteresis area, such as the one observed (−0.06 Pa s^{-1}), presents greater stability. Such an increase suggests interactions between the complex and the surfactant matrix that gently increase the flow resistance without compromising the characteristic rheological behavior, which is desirable for pharmaceutical systems where flow stability and predictability are crucial.[29]

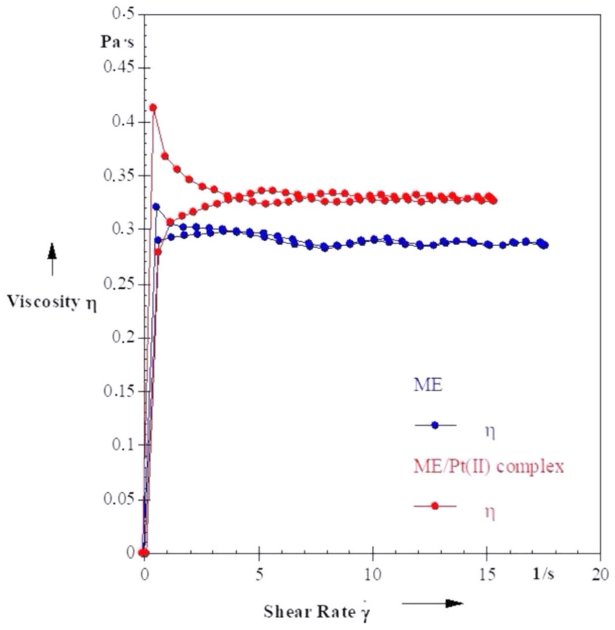

Figure 3. Viscosity curve of the microemulsion (ME) and the Pt^{II} complex associated with the microemulsion (ME/Pt^{II} complex) at 25 °C.

The rheological properties are corroborated by DLS results, which confirm that the Pt^{II} complex is associated with the microemulsion, as indicated by the zeta potential data. These data show variations in the mean particle size, polydispersity index, and zeta potential (see Table 2 and Figures S1-S4, SI section). The average size parameters and the zeta potential in the ME are 165.4 nm and −14.8 ± 5.72 mV, respectively, whereas in the ME/Pt^{II} complex, they are 168.0 nm and −19.2 ± 4.49 mV, respectively. The microemulsions were formed when analyzing particle sizes, which ranged from 10 to 200 nm. Microemulsions with particle sizes between 10 and 200 nm offer significant advantages for drug administration and biological assays due to their ability to cross biological barriers, such as cell membranes and the blood-brain barrier, thereby facilitating targeted delivery of drugs to specific tissues or cells. In addition, they effectively increase the solubility of drugs with low solubility in water or biological fluids, thereby improving bioavailability.[34] Another advantage observed is that in this size range, microemulsions and/or nanoemulsions remain in the bloodstream for a longer time, prolonging their circulation time and, consequently, the effectiveness of the treatment becomes better. Systemic side effects are minimized due to their functionalization, which allows them to be targeted to specific cells or tissues and provides stability to the encapsulated drugs, protecting them from degradation and enabling controlled release. Due to their small size, they are less recognized by the immune system and are more readily eliminated, increasing biocompatibility. In

biological assays, they act as vehicles for biomolecules, probes, or drugs, allowing for precise manipulation and effective monitoring of biological processes.[35,36]

The polydispersity indices of the formulations prepared in this work range from 0.01 to 0.7, indicating monodisperse microemulsions.[37,38] Monodisperse systems with uniformly sized particles are essential in drug administration and biological assays because they ensure consistent, accurate release of the drug or chemical compound being tested, minimizing the risk of adverse effects. The stability of the system is high, with problems such as aggregation and sedimentation avoided, and it ensures a more controlled and effective distribution in tissues, which is crucial for targeted treatments, such as tumors. In addition, this uniformity facilitates the reproducibility of results in trials, making data more reliable and reducing variation in drug delivery, which is vital in therapies that require high precision, such as chemotherapy.[37,38]

The zeta potential measurements aim to analyze the surface charge of the particles. Depending on the charge, these particles can approach each other and merge, destabilizing the microemulsion. Microemulsions or nanoemulsions are considered stable when the zeta potential is between ±30 mV. A value closer to 0 is considered ideal for the stability of the formulations.[39,40] It is important to note that the absolute value of the zeta potential increased from −14.8 mV for the ME to −19.2 mV upon association of the Pt^{II} complex, indicating an increase in the magnitude of the surface charge. This variation is the result of the association of the Pt^{II} complex with the microemulsion, and, according to the variation presented, it can be inferred that the particles of the complex are as if covering the particles of the microemulsion as well as the non-ionic surfactants, which causes a reduction of mobility in addition to reducing the possibility of aggregate formation.[39,41]

The results confirm that the prepared formulations are both thermodynamically and electrostatically stable. This stability protects the system from rapid aggregation, as supported by rheological data showing Newtonian behavior. The low hysteresis area and consistent viscosity across the entire strain rate range indicate that neither large aggregates nor structural changes form, even after the metal complex is incorporated. This stability helps maintain biocompatibility.

Cellular viability

The cell viability assay assesses cell health in response to specific stimuli. This assay employs the acridine orange method, where a fluorescence reaction occurs between the acridine orange dye and the cells. This reaction helps determine the percentage of live and dead cells. This dye interacts with the genetic material, intercalating in the deoxyribonucleic acid (DNA) or ribonucleic acid (RNA) molecules, emitting a green coloration when the cells are alive (viable) and orange in the dead cells (non-viable) (see Figure 4).[15,30,35]

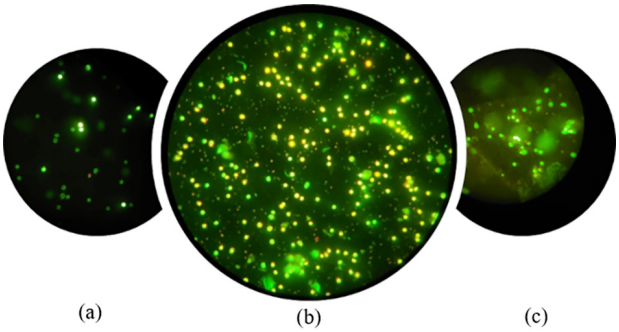

Figure 4. Cell viability assay of peripheral blood mononuclear cells (PBMCs) by the acridine orange method under fluorescence light microscopy at 400× magnification: (a) negative control group (without adding stimuli). (b) Positive control group using lipopolysaccharide. (c) Group with microemulsified ME/Pt^{II} complex.

The cells used in this viability assay were PBMCs, characterized by oval nuclei that can be horseshoe- or kidney-shaped, located at the periphery of the cytoplasm. They have thin, lace-like nuclear chromatin interspersed with small clumps, abundant irregular light blue-gray cytoplasm, and very fine azurophilic granules. PBMCs are part of the immune system and defend the body against infectious agents (viruses, bacteria, and fungi) and tumor cells through phagocytosis. The same cell type was used in phagocytosis assays.[15,42,43]

The viability test of this study showed that both the ME and the Pt^{II} complex associated with the ME showed satisfactory cell viability with percentages of 96.80 ± 2.17 and 97.4 ± 1.34, respectively (Table S1, SI section). These values did not exhibit statistical differences in the viability of the control group (cells only, 98.8 ± 0.45%), indicating that the compound does not harm PBMCs (Figure 5). Other

Table 2. Physicochemical characterization of system microemulsion and associated Pt^{II} complex with microemulsion (ME)

Microemulsion characteristic	Particle size / nm	Polydispersity index	Zeta potential / mV
ME	165.4	0.352	−14.8 ± 5.72
ME/Pt^{II} complex	168.0	0.391	−19.2 ± 4.49

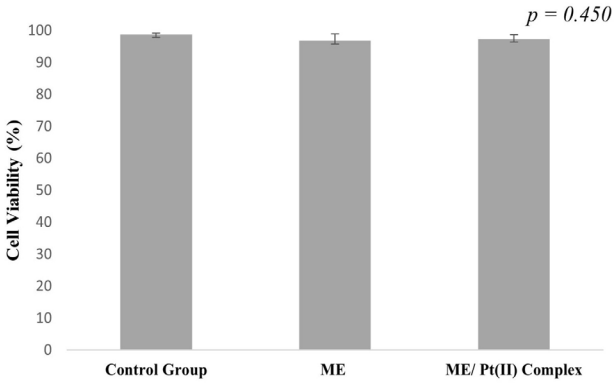

Figure 5. Cell viability study of microemulsion and Pt^{II} complex associated with microemulsion in peripheral blood mononuclear cells (PBMCs). *Analyze significant statistics when the *p*-value is less than 0.05 ($p < 0.05$).

studies[15,44,45] have shown similar results of cell viability with PBMCs, with percentages of 97.83 ± 3.06%.

The study's findings indicate that MEs are compatible with PBMCs and have the potential to serve as effective carriers for compounds with low solubility parameters.

Phagocytosis activity of the mononuclear cells

The phagocytosis index and the microbicidal activity assay were determined using PBMCs (peripheral blood mononuclear cells) stimulated with ME and the Pt^{II} complex associated with ME. The analyses followed the procedures described in the Experimental section, using acridine orange staining. Monocytes, the largest circulating leukocytes, play essential roles in the immune response and the maintenance of tissue homeostasis, primarily through phagocytosis.[46] The phagocytosis index seeks to determine the percentage of phagocytosis events that occur in the presence or absence of a stimulus (Figure 6), where Figure 6A shows the negative control group without stimulation, PBMCs with phagocytosis without bacterial death (blue arrows), PBMCs without phagocytosis events (orange arrows), and PBMCs with phagocytosis events and bacterial death (red arrows). Figure 6B shows the group with microemulsified ME/ Pt^{II} complex (a) dead PBMCs are visualized in orange fluorescence; (b) live PBMCs are identified by green fluorescence; (c) green PBMCs with orange peripheral dots indicate phagocytosis events (highlighted by circles). For the phagocytosis index, no statistically significant differences were observed between the control group (only cells and the EPEC bacterium) and the group containing ME (27.63 ± 6.12 and 24.67 ± 3.79%, respectively) (Figure 7), demonstrating that these are not by themselves capable of stimulating phagocytosis events, thus having no effects on the modulation of PBMCs. The group treated with ME and Pt^{II} complex had a phagocytosis index of 39.25 ± 2.95% (see Table S2, SI section and Figure 7), which was higher than that found in the control group, demonstrating that the Pt^{II} complex associated with ME can induce phagocytosis events and can collaborate with the modulation of the immune response in PBMCs.[15,30]

These results suggest that the association of ME with the Pt^{II} complex was efficient in improving the phagocytosis index of PBMCs and increasing the ability of this association to eliminate phagocytosed microorganisms. Other associations of natural and synthetic compounds with microemulsified systems have been studied to modulate the immune response, whether for antimicrobial or antitumor purposes.[15,47] The ability of microemulsified systems to enhance certain properties is related to improving

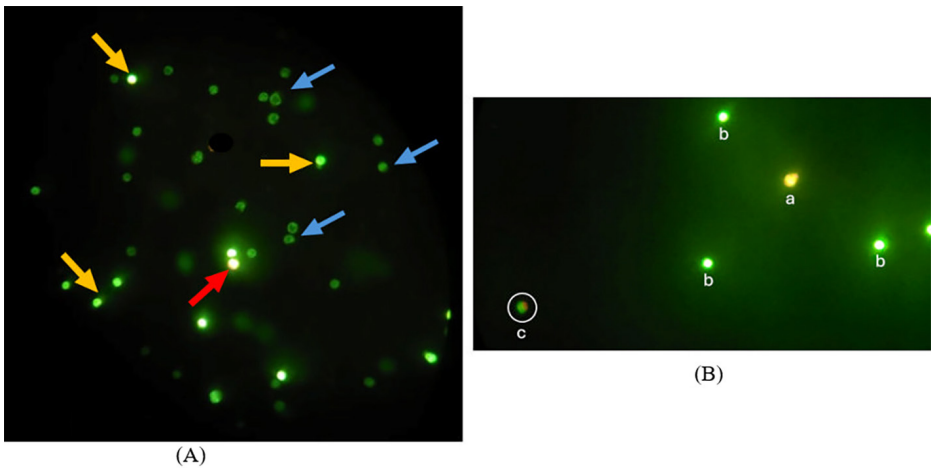

Figure 6. Evaluation of phagocytosis and microbicidal activity in peripheral blood mononuclear cells (PBMCs) and enteropathogenic *Escherichia coli* (EPEC) using the acridine orange method under fluorescence microscopy (400× magnification). (A) negative control group without stimulation, PBMCs with phagocytosis without bacterial death (blue arrows), PBMCs without phagocytosis events (orange arrows), and PBMCs with phagocytosis events and bacterial death (red arrows). (B) The group with microemulsified ME/ Pt^{II} complex (a) dead PBMCs are visualized in orange fluorescence; (b) live PBMCs are identified by green fluorescence; (c) green PBMCs with orange peripheral dots indicate phagocytosis events (highlighted by circles).

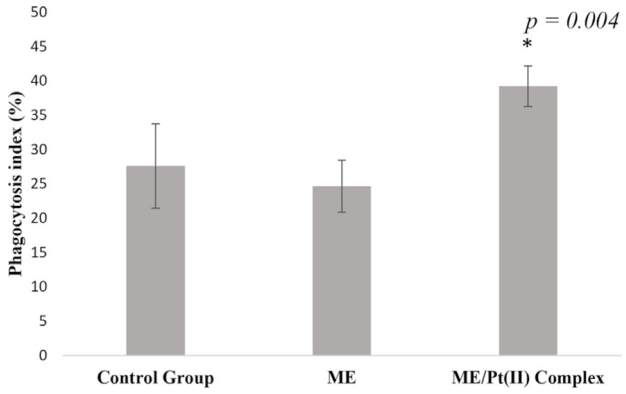

Figure 7. Phagocytosis study of microemulsion and Pt^{II} complex associated with microemulsion in peripheral blood mononuclear cells (PBMCs) in the presence of bacteria *Escherichia coli*. Enteropathogenic (EPEC). *Analyze significant statistics when the *p*-value is less than 0.05 ($p < 0.05$).

parameters such as solubility, degradation, permeation, and, consequently, bioavailability.[15,30,31,47] The results suggest that ME improved parameters such as the solubility of the Pt^{II} complex, increasing its bioavailability and immunomodulatory effects. According to the literature,[48,49] the results obtained may be associated with the ability of the Pt^{II} complex to induce the release of cytokines by immune cells, as well as to produce ROS and stimulate the generation of H_2O_2. These molecules act as essential signaling for phagosome maturation and microbial death. Such redox events modulate intracellular signaling, capable of regulating phagocytic capacity and lysosomal fusion, essential processes for the effective elimination of the pathogen.[50,51] Some studies[31] use biologically active agents as an integral part of the microemulsified system so that they take effect on their own.

Conclusions

The microemulsion, whose formulation consists of SP/TW/BT in the fraction 3.5:5.5:1.0, presented satisfactory HLB, providing stability to the ME. The ME/Pt^{II} complex also showed thermodynamic stability, as indicated by the physicochemical characterizations. Cell viability studies showed values above 95%, indicating that the complex did not present toxicity to PBMCs. Statistically, no significant differences were observed regarding the phagocytosis index. However, it can be noted that the incidence of phagocytosis for the ME/Pt^{II} complex (39.25 ± 2.95%) was slightly higher than the control group (27.63 ± 6.12%) and the group containing only ME (24.67 ± 3.79). These findings suggest that the Pt^{II} complex can trigger phagocytosis events, which can help regulate the immune response in PBMCs, and imply that the Pt^{II} complex could potentially be used in other biological tests, as the ME/Pt^{II} complex's microbicidal activity was higher than that of the ME and control groups.

Supplementary Information

Supplementary information (full characterization of the systems, including particle size and zeta potential images of the microemulsion and Pt^{II}-loaded microemulsion, representative phagocytosis assay images, and tables with cell viability data, phagocytosis indices, and microemulsion composition percentages) is available free of charge at http://jbcs.sbq.org.br as PDF file.

Data Availability Statement

The data that prove the study developed here are available in the text.

Acknowledgements

This work was supported by grants from CNPq, CAPES, and FAPEMAT (Fundação de Amparo à Pesquisa de Mato Grosso, Brazil), 014/2022 – Call for research with a Medium Level of Maturity in Exact and Earth Sciences. The authors are also thankful to the Laboratório de Síntese de Fármacos - LaSFar do Instituto de Química da Universidade Federal de Uberlândia.

Author Contributions

B.A.R. was responsible for data curation, investigation, methodology, formal analysis, conceptualization; A.M.A. for data curation, investigation, methodology, and formal analysis; M.V.A. for conceptualization, data curation, formal analysis, investigation, and methodology; J.A.L.C. R. and W.G. for data curation, investigation, methodology, and formal analysis; E.L.F., A.C.M. C., and W. A.S. for data curation, investigation, methodology, formal analysis, conceptualization, and writing review and editing.

References

1. Rosenberg, B.; Van Camp, L.; Krigas, T.; *Nature* **1965**, *205*, 698. [Crossref]
2. Qi, L.; Luo, Q.; Zhang, Y.; Jia, F.; Zhao, Y.; Wang, F.; *Chem. Res. Toxicol.* **2019**, *32*, 1469. [Crossref]
3. Souza, W. A.; de Almeida, A. M.; Pivatto, M.; de Almeida, M. V.; Guedes, G. P.; Resende, J. A. L. C.; Guerra, W.; *J. Mol. Struct.* **2021**, *1226*, 129250. [Crossref]
4. Farooq, M. A.; Aquib, M.; Farooq, A.; Haleem Khan, D.; Joelle Maviah, M. B.; Sied Filli, M.; Kesse, S.; Boakye-Yiadom, K. O.; Mavlyanova, R.; Parveen, A.; Wang, B.; *Artif. Cells, Nanomed., Biotechnol.* **2019**, *47*, 1674. [Crossref]
5. Prathima, T. S.; Choudhury, B.; Ahmad, M. G.; Chanda, K.;

Balamurali, M. M.; *Coord. Chem. Rev.* **2023**, *490*, 215231. [Crossref]
6. Giorgi, E.; Binacchi, F.; Marotta, C.; Cirri, D.; Gabbiani, C.; Pratesi, A.; *Molecules* **2022**, *28*, 273. [Crossref]
7. Dilruba, S.; Kalayda, G. V.; *Cancer Chemother. Pharmacol.* **2016**, *77*, 1103. [Crossref]
8. Gibson, D.; *J. Inorg. Biochem.* **2021**, *217*, 111353. [Crossref]
9. Wang, M.; You, S. K.; Lee, H. K.; Han, M. G.; Lee, H. M.; Pham, T. M. A.; Na, Y. G.; Cho, C. W.; *Pharmaceutics* **2020**, *12*, 544. [Crossref]
10. Nikolaev, B.; Yakovleva, L.; Fedorov, V.; Li, H.; Gao, H.; Shevtsov, M.; *Pharmaceutics* **2023**, *15*, 1989. [Crossref]
11. Sargazi, S.; Hajinezhad, M. R.; Barani, M.; Mukhtar, M.; Rahdar, A.; Baino, F.; Karimi, P.; Pandey, S.; *Appl. Sci.* **2021**, *11*, 3006. [Crossref]
12. Shah, D. H.; Patel, M. M.; *Int. J. Pharm. Sci. Res.* **2020**, *11*, 2575. [Crossref]
13. Foteeva, L. S.; Trofimov, D. A.; Kuznetsova, O. V.; Kowol, C. R.; Arion, V. B.; Keppler, B. K.; Timerbaev, A. R.; *J. Pharm. Biomed. Anal.* **2011**, *55*, 409. [Crossref]
14. Akartas, I.; Karasulu, H. Y.; *Acta Pol. Pharm. Drug Res.* **2020**, *77*, 183. [Crossref]
15. Ramos, L. C. S.; Torres, A. H. F.; Dalcin, L. D. L.; Silva, K. P. G.; de Freitas, L. G. S.; Fujimori, M.; Fagundes, D. L. G.; França, E. L.; França, A. C. H.; *Adv. Biol. Chem.* **2022**, *12*, 207. [Crossref]
16. Radojevic, I. D.; Petrovic, Z. D.; Comic, L. R.; Simijonovic, D.; Petrovic, V. P.; Hadjipavlou-Litina, D.; *Med. Chem.* **2012**, *8*, 947. [Crossref]
17. de Lacerda, M. L.; Rossi, D. A.; Lourenzatto, E. C. A.; Takeuchi, M. G.; Souza, W. A.; Silva, R. T. C.; Julio, L. G.; Guerra, W.; de Melo, R. T.; *Antibiotics* **2022**, *11*, 1645. [Crossref]
18. Jovičić Milić, S. S.; Jevtić, V. V.; Radisavljević, S. R.; Petrović, B. V.; Radojević, I. D.; Raković, I. R.; Petrović, Đ. S.; Stojković, D. Lj.; Jurišević, M.; Gajović, N.; Petrović, A.; Arsenijević, N.; Jovanović, I.; Klisurić, O. R.; Vuković, N. L.; Vukić, M.; Kačániová, M.; *J. Inorg. Biochem.* **2022**, *233*, 111857. [Crossref]
19. Frei, A.; Ramu, S.; Lowe, G. J.; Dinh, H.; Semenec, L.; Elliott, A. G.; Zuegg, J.; Deckers, A.; Jung, N.; Bräse, S.; Cain, A. K.; Blaskovich, M. A. T.; *ChemMedChem* **2021**, *16*, 3165. [Crossref]
20. Ruan, B.-F.; Guo, Q.-L.; Li, Q.-S.; Li, L.-Z.; Deora, G. S.; Zhou, B.-G.; *Curr. Top. Med. Chem.* **2022**, *22*, 578. [Crossref]
21. de Almeida, A. M.; de Oliveira, B. A.; de Castro, P. P.; de Mendonça, C. C.; Furtado, R. A.; Nicolella, H. D.; da Silva, V. L.; Diniz, C. G.; Tavares, D. C.; Silva, H.; de Almeida, M. V.; *BioMetals* **2017**, *30*, 841. [Crossref]
22. Unadkat, V.; Rohit, S.; Parikh, P.; Sanna, V.; Singh, S.; *Bioorg. Chem.* **2021**, *114*, 105124. [Crossref]
23. Unadkat, V.; Rohit, S.; Parikh, P.; Patel, K.; Sanna, V.; Singh, S.; *Onco. Targets. Ther.* **2022**, *15*, 479. [Crossref]
24. Yadav, N.; Sharma, K.; Sengupta, S.; Singh, S.; *3 Biotech* **2023**, *13*, 413. [Crossref]
25. Mohmad, M.; Agnihotri, N.; Kumar, V.; Azam, M.; Kamal, R.; Kumar, A.; Sharma, U.; Javed, S.; Muthu, S.; Min, K.; *ACS Omega* **2023**, *8*, 31648. [Crossref]
26. Villarreal, W.; Colina-Vegas, L.; Rodrigues De Oliveira, C.; Tenorio, J. C.; Ellena, J.; Fábio, F.; Gozzo, C.; Cominetti, M. R.; Ferreira, A. G.; Antonio, M.; Ferreira, B.; Navarro, M.; Batista, A. A.; *Inorg. Chem.* **2015**, *54*, 11709. [Crossref]
27. Oliveira, C. G.; Romero-Canelón, I.; Silva, M. M.; Coverdale, J. P. C.; Maia, P. I. S.; Batista, A. A.; Castelli, S.; Desideri, A.; Sadler, P. J.; Deflon, V. M.; *Dalton Trans.* **2019**, *48*, 16509. [Crossref]
28. Dell'Anna, M. M.; Censi, V.; Carrozzini, B.; Caliandro, R.; Denora, N.; Franco, M.; Veclani, D.; Melchior, A.; Tolazzi, M.; Mastrorilli, P.; *J. Inorg. Biochem.* **2016**, *163*, 346. [Crossref]
29. Cotrim, A. C. M.; Honorio-França, A. C.; França, E. L.; *Bioint. Res. Appl. Chem.* **2016**, *6*, 1128. [Crossref]
30. Hernandes, M. R. G.; Moraes, L. C. A.; Ribeiro, E. B.; Fagundes, D. L. G.; Honorio-França, A. C.; França, E. L.; *Parasitol. Int.* **2017**, *66*, 299. [Crossref]
31. Prando, W. L. M.; Hoshino, T. T.; Raiser, A. L.; Cavaletti, J. C. S.; Ribeiro, E. B.; Cotrim, A. C. M.; Valladão, D. M. S.; *Braz. J. Biol.* **2023**, *83*, 276545. [Crossref]
32. Pangeni, R.; Poudel, S.; Herz, S. M.; Berkbigler, G.; Duerfeldt, A. S.; Damaj, M. I.; Xu, Q.; *Mol. Pharm.* **2025**, *22*, 1641. [Crossref]
33. Charisis, A.; Kalogianni, E. P.; *Colloids Interfaces* **2023**, *7*, 48. [Crossref]
34. Sharma, A.; Goyal, A. K.; Rath, G.; *J. Drug Target.* **2018**, *26*, 617. [Crossref]
35. Jin, S.; Ye, K.; *Biotechnol. Prog.* **2007**, *23*, 32. [Crossref]
36. Kumar, A. A.; Vine, K. L.; Ranson, M.; *Mol. Pharm.* **2023**, *20*, 2766. [Crossref]
37. Kono, Y.; Sugaya, T.; Yasudome, H.; Ogiso, H.; Ogawara, K.-i.; *Biochem. Biophys. Rep.* **2024**, *38*, 101713. [Crossref]
38. Wu, T.; Chen, K.; He, S.; Liu, X.; Zheng, X.; Jiang, Z.-X.; *Org. Process. Res. Dev.* **2020**, *24*, 1364. [Crossref]
49. Kiromah, N. Z. W.; Sugihartini, N.; Nurani, L. H.; *Pharmacia* **2023**, *70*, 233. [Crossref]
40. Ribeiro, E. B.; de Marchi, P. G. F.; Honorio-França, A. C.; França, E. L.; Soler, M. A. G.; *J. Biomed. Mater. Res., Part A* **2020**, *108*, 234. [Crossref]
41. Oliveira, C. G.; Dalmolin, L. F.; Silva, R. T. C.; Lopez, R. F. V.; Maia, P. I. S.; Moreto, J. A.; *New J. Chem.* **2020**, *44*, 14928. [Crossref]
42. Ziegler-Heitbrock, L.; *Front. Immunol.* **2015**, *6*, 423. [Crossref]
43. Abe, K.; Abe, N.; Sugaya, T.; Takahata, Y.; Fujita, M.; Hayashi, M.; Takahashi, A.; Ohira, H.; *Med. Mol. Morphol.* **2024**, *57*, 110. [Crossref]

44. Cochrane, S.; Rajagopal, R.; Sheffield, D.; Stewart, F.; Hathaway, L.; Barnes, N. M.; Qureshi, O.; Gordon, J.; *Front. Toxicol.* **2024**, *6*, 110. [Crossref]
45. Maciel, L. L. F.; Silva, M. B.; Moreira, R. O.; Cardoso, A. P.; Fernandes, C.; Horn, A.; de Aquino Almeida, J. C.; Kanashiro, M. M.; *Pharmaceutics* **2022**, *14*, 2013. [Crossref]
46. Washington, I. M.; Van Hoosier, G. In *The Laboratory Rabbit, Guinea Pig, Hamster, and Other Rodents*; Suckow, M. A.; Stevens, K. A.; Wilson, R. P., eds.; Elsevier: London, UK, 2012. [Crossref]
47. Torres, A. H. F.; Soares, T. A.; Dalcin, L. D. L.; Rodrigues, G. F. S.; Ribeiro, E. B.; França, A. C. H.; França, E. L.; *Sci. Adv. Mater*. **2021**, *13*, 1538. [Crossref]
48. Gatto, F.; Moglianetti, M.; Pompa, P. P.; Bardi, G.; *Nanomaterials* **2018**, *8*, 392. [Crossref]
49. Yu, J.; Liu, S.; Wang, Y.; He, X.; Zhang, Q.; Qi, Y.; Zhou, D.; Xie, Z.; Li, X.; Huang, Y.; *Bioact. Mater.* **2022**, *7*, 389. [Crossref]
50. Terenzi, A.; Pirker, C.; Keppler, B. K.; Berger, W.; *J. Inorg. Biochem.* **2016**, *165*, 71. [Crossref]
51. Pashkina, E.; Aktanova, A.; Mirzaeva, I.; Kovalenko, E.; Andrienko, I.; Knauer, N.; Pronkina, N.; Kozlov, V.; *Int. J. Mol. Sci*. **2021**, *22*, 7337. [Crossref]

Submitted: August 22, 2025
Accepted Article online: December 16, 2025
Final version online: January 20, 2026